



LJMU Research Online

Gaskell, EE, Ha, T and Hamilton, AR

Ibuprofen intercalation and release from different layered double hydroxides.

<http://researchonline.ljmu.ac.uk/id/eprint/9258/>

Article

Citation (please note it is advisable to refer to the publisher's version if you intend to cite from this work)

Gaskell, EE, Ha, T and Hamilton, AR (2018) Ibuprofen intercalation and release from different layered double hydroxides. Therapeutic Delivery, 9 (9). ISSN 2041-5990

LJMU has developed **LJMU Research Online** for users to access the research output of the University more effectively. Copyright © and Moral Rights for the papers on this site are retained by the individual authors and/or other copyright owners. Users may download and/or print one copy of any article(s) in LJMU Research Online to facilitate their private study or for non-commercial research. You may not engage in further distribution of the material or use it for any profit-making activities or any commercial gain.

The version presented here may differ from the published version or from the version of the record. Please see the repository URL above for details on accessing the published version and note that access may require a subscription.

For more information please contact researchonline@ljmu.ac.uk

<http://researchonline.ljmu.ac.uk/>

Ibuprofen Intercalation and Release from Different Layered Double Hydroxides

Elsie E. Gaskell*¹, Tina Ha¹, Ashley R. Hamilton¹

¹Liverpool John Moores University, school of Pharmacy and Biomolecular Sciences, Liverpool, L3
3AF, UK

* Author of correspondence: Tel.: +44 151 231 2166, e.e.gaskell@ljmu.ac.uk

Structured Abstract

Background: The chemical composition of Layered Double Hydroxides (LDHs) affects their structure and properties. The method of ibuprofen (IBU) intercalation into LDHs may modify its release, reduce adverse effects, and decrease the required dosing frequency.

Methodology: This study investigates the effects of four different LDHs; MgAl-LDH, MgFe-LDH, NiAl-LDH and NiFe-LDH on *in vitro* release of IBU intercalated by co-precipitation and anionic-exchange.

Results: MgAl-LDH was the most crystalline and substitution of either cation decreased LDH order. FT-IR spectra and pXRD confirmed the intercalation of IBU within the lamellar structure of MgAl-LDH and MgFe-LDH. Intercalation of IBU by anion-exchange resulted in slower, partial, drug release compared co-precipitation.

Conclusions: The chemical composition of LDHs affects their crystallinity, IBU intercalation and subsequent release.

Keywords

- Layered double hydroxides
- LDH
- Ibuprofen
- Anionic Exchange
- Co-precipitation
- Drug Release

30 1. Introduction

31 Layered double hydroxides (LDHs) are inorganic lamellar solids often referred to as
32 hydrotalcite-like minerals [1]. They are sometimes referred to as anionic clays due to their physical
33 and chemical similarities with clay mineral [1] but LDHs have anions between octahedral layers [2],
34 whereas clay minerals have cations between octahedral-tetrahedral layers [1].

35 The layers of LDHs are assembled from octahedral sheets of divalent and trivalent metal
36 hydroxides bound together through edge-sharing. The charge imbalance across the sheet,
37 attributed to the di- and trivalent metal cations, results in a net positive charge [2]. LDH sheets can
38 be stacked on top of each other with anions and water molecules between the sheets to
39 counterbalance the positive charge. These interlayer anions are commonly carbonate, halides,
40 nitrates or sulphates [2]. Water molecules and other anionic species can also reside in the
41 interlayer space from the synthesis of the LDH sheets, or through incorporation methods such as
42 anionic-exchange [1]. As expected, the interlayer distance depends on the size, charge and
43 arrangement of the anionic species within the interlayer space [1].

44 The chemical composition of LDHs is generally described as $[M^{II}_{1-x}M^{III}_x(OH)_2][X^{q-}_{x/q} \cdot nH_2O]$,
45 where M^{II} is the divalent cation such as Mg^{2+} , Mn^{2+} , Fe^{2+} , Co^{2+} , Ni^{2+} and M^{III} is the trivalent cation
46 such as Al^{3+} , Mn^{3+} , Fe^{3+} , Co^{3+} , Ni^{3+} [1]. These metal cations must be of similar ionic radius to
47 Mg^{2+} ions to be able to fit in the brucite-like ($Mg(OH)_2$) layers [1]. Additionally, it has been
48 suggested that the charge density ($M^{III}/(M^{II}+M^{III})$) which relates to the anionic exchange capacity
49 must be between 0.2 and 0.33, with the M^{II}/M^{III} ratio being between 2 and 4.37 to get a pure LDHs
50 structure [2]. The chemical variation of LDHs is diverse due to the possible ratios and combinations
51 of divalent and trivalent cations, in addition to the choice of anions that can be incorporated
52 between the layers [3]. Moreover, preparations of LDHs containing quaternary and monovalent
53 cations have also been reported [4,5].

54 LDHs can act as drug carriers due to their positively charged layers and interlayer anions that
55 can be exchanged for negatively charged drug compounds for storage and subsequent release in a
56 controlled manner [6,7]. Current developments in drug-delivery systems strive to optimise drug-
57 release by means of maintaining a therapeutic concentration of the drug at the targeted site for an
58 extended period of time, thus prolonging the therapeutic effects, reducing the dosing frequency
59 and minimising dose-related adverse effects [3]. Recent years have seen a growing interest in the

60 pharmaceutical applications of LDHs as controlled drug delivery systems [4,8]. LDH chemical
61 composition affects the layer structure and properties, which affects the intercalation and release
62 of drug molecules [9]. Therefore, it is possible to optimise the chemical composition of LDHs to
63 design controlled release drug nanocarriers that are also biocompatible *in vivo* [10,11].
64 Furthermore, the application of LDH materials in the biomedical field expands beyond their
65 nanoparticle drug carrying properties and includes, amongst other applications, the use of LDHs in
66 biomaterials for tissue engineering [12] and applications as biosensors [13], as well as formulation
67 into hybrid polymer containing nanocomposite hydrogels [14], films [15] and beads [16].

68 The most common intercalation methods described are co-precipitation (co) and anionic-
69 exchange (ex) [4] but can also be achieved through reconstruction, hydrothermal precipitation and
70 transformation methods [4,17,18]. These intercalation methods produce different LDH-drug
71 composites in terms of their structure, bonding, purity and amount of intercalated drug [19], which
72 consequently influence drug release rate and characteristics [20].

73 LDHs offer many advantages as drug carriers due to a high adsorptive capacity, low toxicity [1],
74 ability to improve drug stability [21], and being easy and inexpensive to prepare. In recent years,
75 LDHs have been used to successfully intercalate many drugs and biomolecules including anti-
76 inflammatory drugs [3,4], antihypertensive drugs [22], antimicrobials [23], anticancer drugs [24],
77 and DNA fragments [25].

78 Non-steroidal anti-inflammatory drugs (NSAIDs) are a class of molecules indicated for the
79 treatment of pain and inflammation [26]. However, these drugs are limited by their low water
80 solubility [27] which can restrict their dissolution and absorption in the body. A study on naproxen
81 and flurbiprofen showed a substantial increase in water solubility and improved drug
82 bioavailability when intercalated within MgAl-LDH [19]. Similarly, Capsoni *et al.* found that co-
83 precipitating carprofen with Zn₂Al-LDH significantly increased the drugs solubility potentially
84 improving subsequent absorption [28]. The solubility of NSAIDs are also increased when LDHs
85 were included as additives, but to a lesser extent than when intercalated within the layers [29].
86 Furthermore, the LDH layers can also act as a barrier and provide gastrointestinal protection
87 against the adverse effects of NSAIDs [30].

88 Several studies also demonstrated that LDHs can modify and prolong the release of the
89 intercalated NSAIDs [3,4]. For example, Ambrogi *et al.* intercalated ibuprofen (IBU) into MgAl-LDH

90 and observed slower *in vitro* release compared to the commercial formulation [31]. Li *et al.*
91 revealed that the dissolution of fenbufen was slower when intercalated by co-precipitation in
92 MgAl-LDH and MgLi-LDH [32]. However, the MgAl-LDH was concluded to be the more effective
93 delivery system as its release rate was significantly slower. The chemical composition of LDHs affect
94 drug intercalation. For example, del Arco *et al.* showed that fenbufen intercalated successfully in
95 MgAl-LDH via co-precipitation, anionic exchange, and reconstruction but it was only intercalated
96 into MgAlFe-LDH by co-precipitation and anionic-exchange [3]. Subsequently, MgAl-LDH released
97 its intercalated drug fully while MgAlFe-LDH released 93% of its intercalated drug at a slower rate
98 [29].

99 Another study revealed that the release rate of naproxen decreased when the charge density
100 of the LDHs delivery system increased [33]. Williams and O'Hare suggested that the release of
101 NSAIDs from LDHs is affected by the pH of the release medium, demonstrating a slower release at
102 pH 7 than at pH 4 due to acidity causing hydrolysis of the LDH sheets [9]. Additionally, the impact
103 of interlayer space size on drug loading and subsequent release has been demonstrated by
104 Djaballah *et al.* [5] who demonstrated suitability of the very short interlayer space in ZnTi-LDH to
105 deliver low-dose therapy of intercalated IBU.

106 These studies show that the intercalation of NSAIDs into LDHs for a modified release system
107 depends on multiple factors, including the chemical composition and charge density of the LDHs,
108 the intercalation method and the pH of the release medium. These variables collectively influence
109 the LDH structure and orientation of the drug molecules within the interlayer space, which will
110 consequently affect the rate and amount of drug released. Williams and O'Hare suggest it is
111 possible to optimise these factors to obtain an optimal modified release formulation of the drug,
112 although these have not yet been fully investigated [9]. Current interests include further improving
113 the drug delivery potential of LDHs and research into this had included surface coating the drug
114 loaded LDH nanoparticles with mesoporous silica [34].

115 The aim of this work was to investigate and characterise the effects of four different metal
116 compositions of LDH sheets (MgAl-LDH, MgFe-LDH, NiAl-LDH and NiFe-LDH) on the intercalation
117 and *in vitro* drug-release of IBU using two different intercalation methods: co-precipitation and
118 anionic-exchange.

119 2. Materials and Methods

120 2.1 LDH-IBU composite preparation

121 2.1.1. Co-precipitation of LDH-IBU composites

122 Co-precipitation (co) was used to prepare the following four metal compositions of LDH-IBU
123 composites: MgAl-LDH-IBU(co), MgFe-LDH-IBU(co), NiAl-LDH-IBU(co), and NiFe-LDH-IBU(co).

124 This involved preparing the relevant metal salts solution (molar ratio metal ion²⁺/metal ion³⁺
125 =1:2) [31]. Firstly, 0.025 mol of divalent metal chloride salt (MgCl₂ or NiCl₂) and 0.0125 mol of
126 trivalent metal chloride salt (AlCl₃ or FeCl₃) were dissolved in 50 mL of deionised water. Secondly, a
127 caustic solution of the drug was prepared by dissolving 0.0125 mol of IBU into a solution
128 containing 5 M NaOH (3 mL) and deionised water (50 mL).

129 The metal salts solution was added dropwise from a burette into a stirring caustic solution of
130 IBU. Additions of 5 M NaOH solution were made as necessary to maintain the mixture at pH 9. The
131 exact volume of 5 M NaOH (8 – 14mL) solution added was recorded to establish the final volume
132 of the resultant mixture. Once all of the metal salts solution was added, the viscous resultant
133 mixture was left to stir for one hour following which it was centrifuged at 25000 rpm for 20
134 minutes and the pellets were dried. After drying, the solid products were grounded into fine
135 particles using a mortar and pestle, and the weights of the solids were recorded and the yields
136 calculated according to the following equation:

$$137 \text{ Yield (\%)} = \frac{\text{mass of LDH obtained (g)}}{\text{total mass of metal salts and IBU used (g)}} \times 100$$

138 The supernatant was kept to assay the amount of IBU not intercalated, as detailed in section
139 2.3 below.

140

141 2.1.2 Anionic-exchange of LDHs with IBU

142 The anionic exchange (ex) method was used to prepare the following four metal compositions
143 of LDH-IBU composites: MgAl-LDH-IBU(ex), MgFe-LDH-IBU(ex), NiAl-LDH-IBU(ex) and NiFe-LDH-
144 IBU(ex).

145 This involved a two-step process; the first step involved the co-precipitation of MgAl-LDH,
146 MgFe-LDH, NiAl-LDH and NiFe-LDH exactly as detailed above, but excluding the IBU in the caustic
147 solution. The second step involved equilibrating 1 g of the LDHs with 2 g of IBU dissolved in a

148 solution containing 5 M NaOH (10 mL) and deionised water (74 mL). This mixture was covered with
149 foil paper, heated to 60 °C [31] and stirred vigorously on a hotplate stirrer for 3 hours. After 3
150 hours, the mixture was left to cool before centrifuging at 25000 rpm for 20 minutes. After
151 centrifugation, the pellets were dried the solid products were grounded into fine particles using a
152 mortar and pestle, and the weights of the solids were recorded. The supernatant (3 mL) was kept
153 to assay the amount of IBU not intercalated, as detailed in section 2.3.

154

155 **2.1.3 Preparation of the physical mixes**

156 Different metal salts and IBU were mixed together in a mortar and pestle to prepare physical
157 mixes equivalent to each of the LDHs synthesised. The amounts used reflected the 2:1 ratio of the
158 divalent and trivalent metal salts. Additionally, the amount of IBU used was equivalent to the
159 amount of IBU determined from the co-precipitated LDH-IBU composites (section 2.3).

160

161 **2.2 Characterisation of LDH-IBU composite**

162 The composites were analysed on a Perkin Elmer Spectrum 1000 Fourier-Transform Infrared
163 (FT-IR) Spectrophotometer with a Pike Miracle ATR attachment in the range of 4000 to 600 cm⁻¹.
164 The power X-ray diffractograms (pXRD) of the composites were collected on a Rigaku Mini-Flex X-
165 ray diffractometer using Cu K α radiation of wavelength 1.54 Å in the scan range 2 θ : 3° to 30°.

166 The LDHs and LDH-IBU composites were analysed using FT-IR spectroscopy and pXRD. The
167 physical mixes were analysed using FT-IR spectroscopy only.

168

169 **2.3 Determination of amount of IBU intercalated**

170 All UV analysis was completed on the Thermo Spectronic Genesys 10 UV-Visible
171 Spectrophotometer at wavelength 265 nm.

172

173 **2.3.1 Back-exchange method (carbonate-ion exchange)**

174 The amount of IBU intercalated into each LDH-IBU composite was determined by carbonate-
175 ion back-exchange. This involved exchanging higher affinity carbonate ions with intercalated IBU,
176 thus releasing the drug out of the LDHs for quantifying with UV spectroscopy.

177 0.005 mol sodium carbonate decahydrate (1.4307 g) was dissolved in phosphate buffered

178 saline (50 mL, pH 7.4). This mixture was heated to 80 °C before adding 500 mg of LDH-IBU. Then,
179 the mixture was sealed with foil, stirred and maintained at 80 °C for 4 hours using a magnetic
180 hotplate stirrer. When cooled to room temperature, 3 mL of the mixture was pipetted out,
181 centrifuged and its supernatant was analysed in a quartz cuvette under UV spectroscopy at 265 nm
182 to determine the mass of IBU released from 500 mg of LDH-IBU. This was then used to calculate
183 the amount of IBU loaded into the various composites using the following equation:

$$184 \quad \text{IBU loading (mg/g LDH)} = \frac{\text{mass of IBU determined by back - exchange (mg)}}{\text{mass of LDH used in back - exchange(g)}}$$

185

186 **2.3.2 IBU intercalation efficiency**

187 The amount of IBU not intercalated into the various composites was determined by
188 measuring the amount of IBU remaining in the supernatant of the intercalation mixture after
189 centrifugation. The supernatant was analysed in a quartz cuvette under UV spectroscopy at 265
190 nm to determine the mass of IBU not intercalated. This was deducted from the initial mass of IBU
191 added and used to calculate the percentage intercalation efficiency using the following equation:

$$192 \quad \text{IBU intrcalation efficiency (\%)} \\ 193 \quad = \frac{\text{mass of IBU used (mg)} - \text{mass IBU not intercalated (mg)}}{\text{mass of IBU used (mg)}} \times 100$$

194

195 **2.4 In vitro drug release**

196 A sample of each physical mix and co-precipitated and anion exchanged LDH-IBU composite
197 (230 mg) was suspended in separate round-bottom flasks containing phosphate buffer saline (PBS,
198 200 mL, pH 7.4) under constant stirring, in an incubator at a constant physiological temperature
199 (37 ± 5 °C). The mass of the sample suspended was equivalent to approximately 100 mg of IBU, as
200 estimated from the preliminary back-exchange. This mass/volume ratio was chosen to correspond
201 to the sink conditions, based on the solubility of IBU at pH 7.4 [31].

202 Once, the samples were suspended, aliquots (1 mL) of dissolution medium were taken at 5
203 minutes interval up to one hour. The aliquots were then centrifuged and their supernatant were
204 analysed under UV spectroscopy at 265 nm. One millilitre of PBS was replaced after each aliquot
205 sample was removed to maintain sink conditions. The dissolution tests were repeated and the
206 average absorbance values were used to determine the concentration of IBU released.

207 The amount of IBU released was calculated as a percentage over the total amount of IBU in

208 230 mg of the physical mix, or the total amount of intercalated IBU in 230 mg of LDH-IBU
209 composite.

210

211 3. Results and Discussion

212 3.1 Intercalation of IBU in LDHs by co-precipitation and anionic-exchange

213 During the co-precipitation of LDHs a pH of 9 was maintained. This alkaline environment was
214 required to create a supersaturated conditions for the hydroxide ions to displace the metal salts
215 and form a precipitate [35]. Precipitation occurred when the NaOH solution was added into
216 mixtures of metals salts with and without IBU. However, a larger addition of NaOH solution was
217 generally required to maintain pH 9 during the co-precipitation of LDHs with IBU due to the acidic
218 nature of IBU [20].

Table 1. Yield of LDHs prepared without ibuprofen (IBU) and via co-precipitation with IBU.

LDH composite	Yield (%) with no IBU	Yield (%) co-precipitated with IBU
MgAl-LDH	85	79
MgFe-LDH	71	65
NiAl-LDH	70	62
NiFe-LDH	77	60

219

220 Co-precipitation of LDHs with IBU produced a lower yield than without IBU (table 1). This
221 indicates that LDHs form more easily with chloride anions than IBU anions, which suggests that the
222 presence of IBU disrupts the formation of LDH layers due to its relatively larger size and hydrophobic
223 nature. Bulky anions are capable of moving the layers out of alignment as a consequence of the
224 turbostratic effect [2], thus less layers can be assembled during co-precipitation. Additionally,
225 MgAl-LDH and co-precipitated MgAl-LDH-IBU had a higher yield compared to the other co-
226 precipitated composites. This indicates that these metal ions are more efficient in forming LDHs,
227 which was expected as MgAl-LDHs have a similar composition to the natural mineral hydroxycalcite
228 [4].

229 The co-precipitation process resulted in considerably higher IBU intercalation efficiencies than
230 anionic-exchange (table 2). This is likely due to the varying intercalation mechanism, as explained

231 below with the difference in interlayer spacing. Similar findings have been reported by other
 232 groups, Djebbi *et al.* describe a lower adoption of berberine chloride into MgAl-LDH prepared by
 233 ion-exchange compared to equivalent co-precipitation methods [36].

234

Table 2. Ibuprofen (IBU) intercalated

	co-precipitated (co)				anion-exchanged (ex)			
	MgAl- LDH- IBU(co)	MgFe- LDH- IBU(co)	NiAl- LDH- IBU(co)	NiFe- LDH- IBU(co)	MgAl- LDH- IBU(ex)	MgFe- LDH- IBU(ex)	NiAl- LDH- IBU(ex)	NiFe- LDH- IBU(ex)
	IBU intercalation efficiency (%)	90.31	87.98	76.36	58.14	29.50	27.50	25.50
IBU loading (mg/g LDH composite)	420	490	396	314	368	342	296	252

235 In both methods, MgAl-LDH and MgFe-LDH intercalated more IBU than NiAl-LDH and NiFe-
 236 LDH, which may be due to the increased order and crystallinity of MgAl-LDHs and MgFe-LDH
 237 compared to Ni containing LDH (see section 3.4). Ambrogi *et al.* (2001) reported to have achieved
 238 an IBU content of 50% by anionic exchange. MgAl-LDH was also reported to have intercalated
 239 fenbufen with a drug content of 51% when co-precipitated at pH 8, and 61% when precipitated at
 240 pH 13 [32]. This indicates that more drug molecules are intercalated at higher basicity, as the layers
 241 are more regular [32].

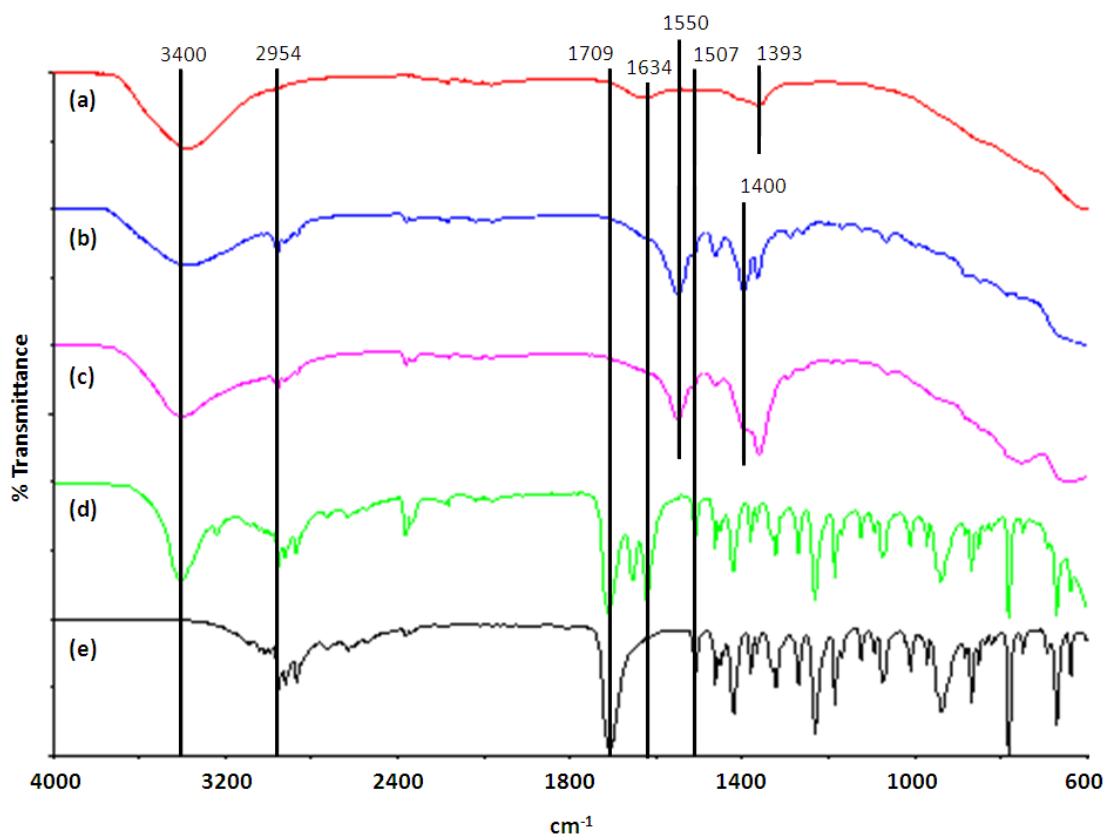
242 The IBU loading in the various composites (table 2) was deduced from the amount of IBU
 243 back-exchanged. In both types of composite materials (co-precipitated and ion exchanged) there
 244 was residual drug remaining on the LDHs that was not released during the back-exchange.
 245 However it is notable that IBU was relinquished from the anion-exchange prepared composites
 246 more readily, which suggests a stronger adsorption of IBU in the co-precipitated LDH composites.

247

248 3.3 Characterisation of LDHs and physical mixes with FT-IR spectroscopy

249 The FT-IR spectrum of IBU (figure 1e) consists of the characteristic C=O stretching vibrations
 250 at⁻¹ due to the free carboxylic acid group, the C-H alkyl stretching at 2954-2868 cm⁻¹ due to the
 251 aliphatic C-H groups [37], and the skeletal stretching vibrations between 1507-1418 cm⁻¹ due to
 252 the C-C bonds in the aromatic ring [38]. These characteristic absorptions were also observed in the

253 physical mixes (figure 1d), suggesting that simply mixing IBU with the metal salts or LDHs does not
254 result in intercalation. The FT-IR spectra of LDHs (figure 1a) display weak peaks at 1393-1357 cm^{-1}
255 indicating the presence of carbonate [3] and implies that carbonate anions were adsorbed onto
256 the LDHs from the atmosphere and dispersion media due to their strong affinity [2].
257



258
259 **Figure 1.** FT-IR spectra of (a) the MgAl-LDH synthesised, (b) the co-precipitated MgAl-LDH-IBU, (c)
260 the anion-exchanged MgAl-LDH-IBU, (d) a physical mix of MgCl_2 , AlCl_3 and IBU and (e) IBU
261

262 The aliphatic C-H stretching was present on the spectra of the physical mix sample and LDH-
263 IBU composites (figures 1b, c and d), but not of the LDHs without IBU (figure 1a). This establishes
264 the presence of IBU in the physical mixes and LDH-IBU composites. The LDHs and LDH-IBU contain
265 OH groups as shown by the broad FT-IR peak between 3400 and 3335 cm^{-1} relating to the hydroxyl
266 groups within the LDH layers, and to the interlayer and adsorbed water [39]. The bending modes
267 of OH bonds are only seen on the spectra of LDHs at 1634-1629 cm^{-1} , as there are no IBU
268 molecules to obscure it. The broadening of the OH stretching peak indicates that OH groups are
269 hydrogen bonded [38].

270 The FT-IR absorption due to the free acid group of IBU is no longer visible on the spectra of
 271 LDH-IBU composites, confirming immobilisation of IBU onto the surface of LDHs. FT-IR absorption
 272 modes due to the asymmetric and symmetric stretching of the carboxylate anion group (COO^-) are
 273 seen at $1556\text{-}1528\text{ cm}^{-1}$ and $1408\text{-}1360\text{ cm}^{-1}$, respectively (table 3). This implies that the negatively-
 274 charged carboxyl group of IBU interacts with the positively charged layers of the LDHs. Similar
 275 changes in FT-IR spectra were reported with the intercalation of fenbufen [32] and indomethacin
 276 [37,40] into MgAl-LDH. Conversely, it was observed by del Arco *et al.* that this change did not occur
 277 with the intercalation of meclofenamic acid into MgAl-LDH because its sodium salt was used [3].

278 The FT-IR spectra of the LDH-IBU composites were similar (figure 2), which suggests that IBU
 279 interacts with these LDHs in the same manner regardless of intercalation method or LDH
 280 composition. The carbonyl stretching from IBU disappears in both the LDH-IBU composites and the
 281 COO^- peaks occur at similar wavelengths. In addition, the FT-IR absorbance modes for the LDHs
 282 remained in their original positions, indicating the structure of the LDHs remained unchanged
 283 during and after the intercalation of IBU.

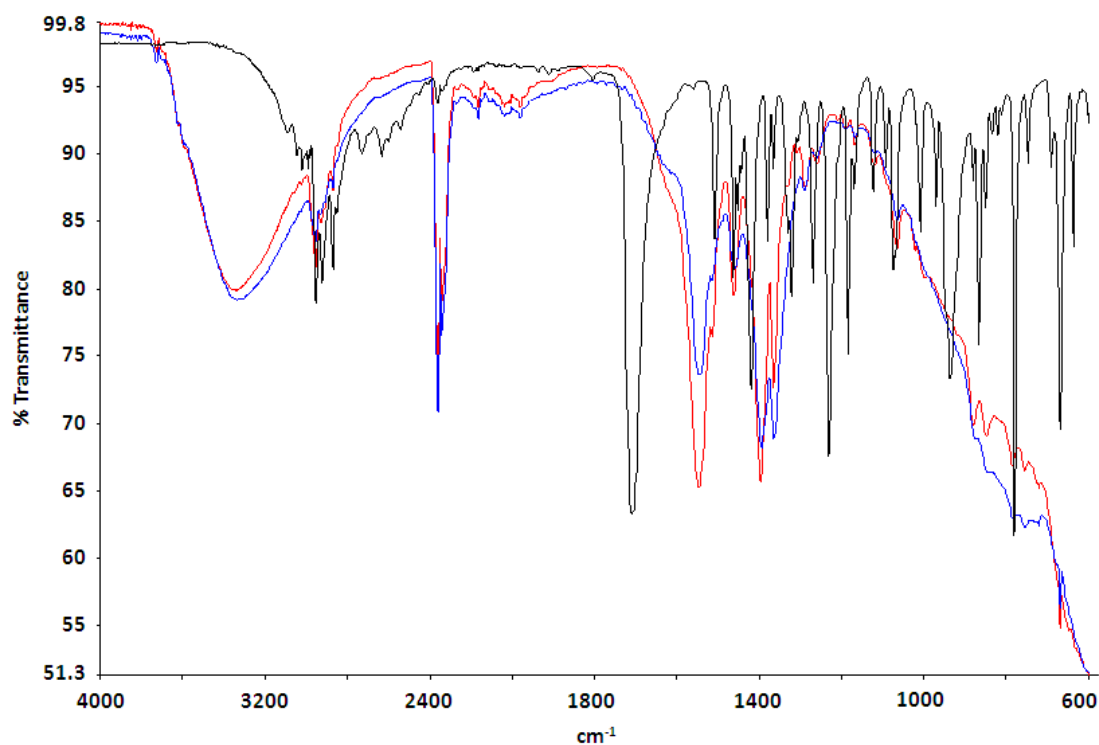
284
 285
 286

Table 3. Absorption peaks of interest on the FT-IR spectra of ibuprofen (IBU), co-precipitated (co) LDH-IBU and anion-exchanged (ex) LDH-IBU composites.

	FT-IR absorption peaks (cm^{-1})		
	$\nu(\text{C=O})$	$\nu_{as}(\text{COO}^-)$	$\nu_s(\text{COO}^-)$
IBU	1709, s, sh	-	-
MgAl-LDH-IB(co)	-	1548, s, sh	1396, s, sh
MgFe-LDH-IBU(co)	-	1552, s, sh	1408, s, sh
NiAl-LDH-IBU(co)	-	1546, s, sh	1397, s, sh
NiFe-LDH-IBU(co)	-	1548, s, sh	1395, s, sh
MgAl-LDH-IBU(ex)	-	1548, m, sh	1362, s, sh
MgFe-LDH-IBU(ex)	-	1556, m, sh	1361, s, sh
NiAl-LDH-IBU(ex)	-	1542, m, sh	1363, s, sh
NiFe-LDH-IBU(ex)	-	1538, m, sh	1360, s, sh

s = strong, m = medium, sh = sharp, ν_s = symmetrical stretching, ν_{as} = asymmetrical stretching

287
 288



289

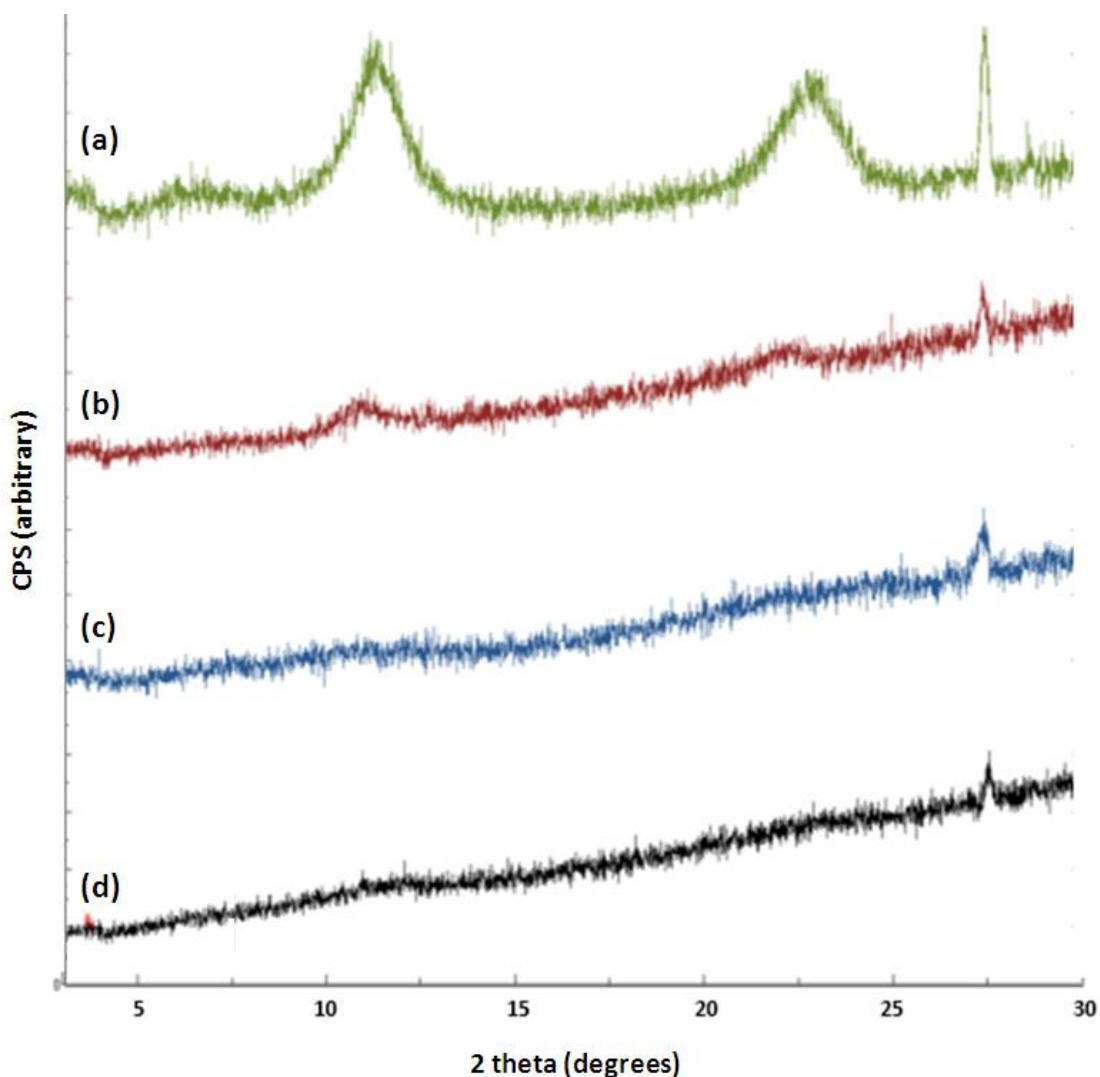
290 **Figure 2.** FT-IR spectra of co-precipitated (co) NiAl-LDH-IBU(co) (red), anion-exchanged (ex) NiAl-
 291 LDH-IBU(ex) (blue) and ibuprofen (IBU) (black).

292

293 **3.4 Characterisation of LDHs with pXRD**

294 MgAl-LDH was the most crystalline structure, followed by MgFe-LDH, NiAl-LDH and NiFe-LDH
 295 in descending order of crystallinity, with the latter two materials showing no observed diffraction
 296 at around 11 deg. 2θ (figure 3). This implies that the two Mg-containing materials are laminar
 297 crystalline LDH structures and whereas the two Ni-containing materials have formed amorphous
 298 metal oxides. This is due to the charge to size ratio of the metal ions which affects the layer charge
 299 density [41], and therefore influences the stacking of the layers. These data suggest the
 300 combination of magnesium and aluminium cations produce superior layer charge density than the
 301 other metal combinations. This finding is also supported by the existence of the only natural LDH,
 302 hydrotalcite, which consists of magnesium and aluminium ions [41]. The high crystallinity of MgAl-
 303 LDH would also explain its high yield compared to the other LDHs (table 1).

304



305

306 **Figure 3.** Diffractograms of synthesised LDHs (a, green) MgAl-LDH, (b, red) MgFe-LDH, (c, blue)
 307 NiAl-LDH, and (d, black) NiFe-LDH

308

309 The method of synthesis affects the crystallinity of the LDHs, and consequently the orientation
 310 of IBU within the interlayer space. MgAl-LDH has a d_{003} value of 0.778 nm (table 4) which
 311 represents the size of one cationic layer and the interlayer space and is consistent with other LDHs
 312 reported in the literature [31,42]. Upon intercalation of IBU by co-precipitation and anionic
 313 exchange, the d_{003} value increased by 1.627 nm and 1.564 nm, respectively, demonstrating
 314 placement of IBU within the interlamellar space. This increase in interlayer space is similar to that
 315 seen with other organic anions of a similar size to IBU, such as fenbufen [32] and indomethacin
 316 [40].

317

Table 4. Characteristics of peak d_{003} on the diffractograms of the LDHs, co-precipitated LDH-IBU composites and anionic-exchanged LDH-IBU composites.

LDHs composite	d_{003} (nm) for LDH	d_{003} (nm) for LDHs co-precipitated with IBU	d_{003} (nm) for LDHs anionic-exchanged with IBU
MgAl-LDH	0.778	2.405	2.342
MgFe-LDH	0.796	2.425	0.796
NiAl-LDH	No diffraction	2.425	No diffraction
NiFe-LDH	No diffraction	No diffraction	No diffraction

318

319 Additionally, the increase in d-values for MgAl-LDHs containing IBU suggest that IBU formed
 320 a tilted bilayer between the layers [41], with its carboxylate groups interacting with the cationic
 321 surface and its primary axes perpendicular to the layers [32]. This arrangement has also been
 322 reported with the co-precipitation of ketoprofen and MgAl-LDH, which produced a similar
 323 expansion of the interlayer spacing by 1.72 nm [38].

324 The orientation of IBU occupies less interlayer space when intercalated via anionic-exchange
 325 than co-precipitation, as evident by the difference in expansion of interlayer space (table 4). This is
 326 likely because the co-precipitation allows the formation of hydroxides layers around IBU molecules,
 327 which would therefore encapsulate more anions, and widen the initial interlayer space. However,
 328 anionic-exchange intercalates IBU into LDHs that already contains small chloride anions in the
 329 interlayer space, which can inhibit absorption, hence reduced yield, and expansion of the
 330 interlayer space.

331 After intercalation of IBU via anion exchange into MgAl-LDH, the d_{003} reflection became more
 332 intense and sharper (diffractograms not shown). This suggests that the MgAl-LDH layered structure
 333 became more ordered after intercalation. The d_{003} reflection of co-precipitated MgAl-LDH-IBU
 334 composite is less intense than that of the MgAl-LDH and anionic exchanged MgAl-LDH-IBU
 335 equivalents, suggesting that co-precipitation produces LDH-IBU composites that are less ordered.
 336 This implies that IBU disrupts the stacking of the cationic layers during co-precipitation, which does
 337 not occur with anionic-exchange process as the LDH layers are already formed and associated
 338 before the intercalation of IBU. Huang *et al.* report an improved crystal structure when IBU-LDH
 339 materials are prepared by the hydrothermal precipitation method compared to the traditional co-
 340 precipitation method also applied in this study [43] implying that harsher conditions are required

341 to overcome the issue of IBU hindering the formation of ordered layers.

342 MgFe-LDH exhibit basal reflections that are very broad, asymmetrical and have a low intensity
343 (figure 3b) and represents a poorly crystalline structure with minimal layers [38]. The interlayer
344 spacing is found to be 0.796 nm, which is the same value for MgFe-LDH reported by Gasser [44].
345 Magnesium and iron cations are not as efficient at forming structured LDHs as magnesium and
346 aluminium cations under the same synthesis conditions. This is shown by the weaker reflections
347 compared to MgAl-LDH, which is likely due to iron cations being larger than aluminium cations
348 [45], which could create distortions within the cationic LDH layers [41].

349 Similarly, on intercalation of IBU into MgFe-LDH by co-precipitation, the interlayer space
350 increased by 1.629 nm. This confirms the successful intercalation of IBU by co-precipitation, as the
351 interlayer space expanded by the same distance as with the intercalation of IBU in MgAl-LDH. It
352 also suggests that MgFe-LDH-IBU has the same bilayer arrangement of IBU as MgAl-LDH-IBU.
353 Again, the reflections of MgFe-LDH-IBU(co) are less intense than MgAl-LDH-IBU(co) due to the
354 distortion caused by the larger aluminium cations.

355 On the contrary, the intercalation of IBU into MgFe-LDH by anionic-exchange was
356 unsuccessful, as the d_{003} value remained the same. This could be due to the irregular structure of
357 the MgFe-LDH making it challenging for IBU to intercalate. Although, IBU did not intercalate into
358 MgFe-LDH, its FT-IR spectra indicate that IBU still formed bonds with the LDH, meaning IBU was
359 adsorbed onto the outer surfaces of the LDH particles.

360 The diffractograms of NiAl-LDH and NiFe-LDH do not exhibit any diffractions around 11 deg.
361 2θ , thus an ordered layered structure was not formed. Nickel cations have a smaller ionic radius
362 than magnesium cations [45], which increases its charge density and makes them more strongly
363 bound to chloride anions; requiring more vigorous method to successfully synthesise nickel
364 containing LDHs [46,47]. NiAl-LDH and NiFe-LDH have previously successfully been prepared using
365 the co-precipitation method however the intercalation anion was carbonate [48,49] suggesting
366 that chloride anions are not conducive to LDH formation for nickel containing materials.

367 As a lamellar structure was not formed, the intercalation of IBU by anionic-exchange was
368 unsuccessful for both NiAl-LDH and NiFe-LDH, as evident from the absence of reflections in these
369 diffractograms. While the intercalation of IBU into NiFe-LDH by co-precipitation was also
370 unsuccessful, the pXRD analysis suggests that NiAl-LDH was able to intercalate IBU by co-

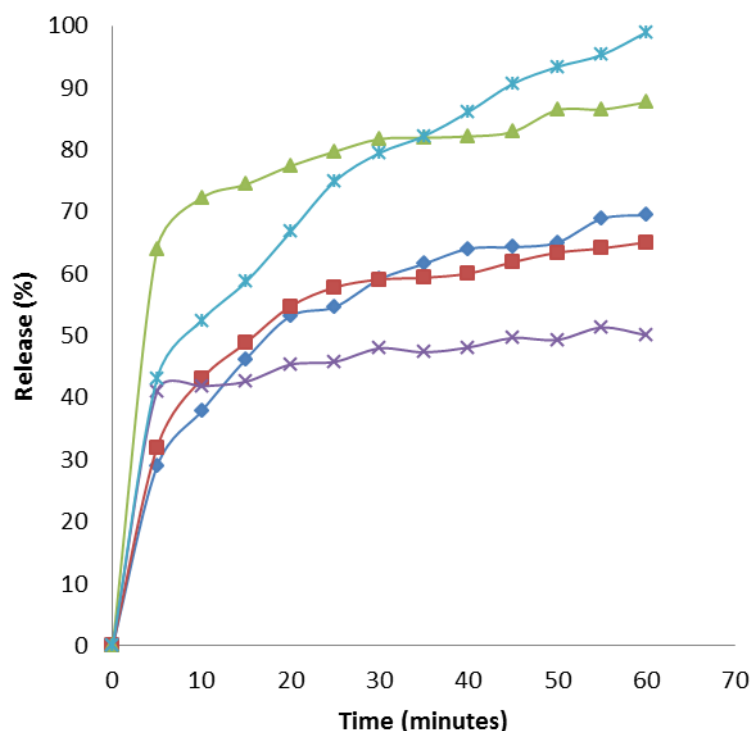
371 precipitation as it had an interlayer space of 2.425 nm. This value is similar to the other IBU co-
372 precipitated LDHs in this study (MgAl-LDH-IBU and MgFe-LDH-IBU), which suggest that a bilayer of
373 IBU had formed. In turn, this suggests IBU anions help the formation of the layered structure,
374 which could not be formed with chloride anions alone.

375

376 3.5 *In vitro* drug release

377 The IBU release profiles in phosphate buffer saline (pH 7.4) from co-precipitated and ion-
378 exchanged LDH-IBU was performed on the five LDHs showing d_{003} reflections on their
379 diffractograms (figure 4). The IBU release profile differed for each LDH-IBU composite tested
380 showing that differences in LDH chemical composition and IBU intercalation method also affected
381 the final drug release behaviour. The physical mixes of the parent LDHs (MgAl-LDH, MgFe-LDH and
382 NiAl-LDH) and IBU did not show release profiles (data not shown) as all the IBU present in the mix
383 had dissolved once suspended in the phosphate buffer saline.

384



385

386 **Figure 4.** Drug release profiles of ibuprofen (IBU) from LDH-IBU composites of co-precipitated (co)
387 MgAl-LDH-IBU(co) (dark blue diamonds), MgFe-LDH(co) (green triangles), and NiAl-LDH-IBU(co)
388 (light blue asterix), and anionic-exchanged (ex) MgAl-LDH-IBU(ex) (red squares) and MgFe-LDH-
389 IBU(ex) (purple crosses).

390 All the LDH-IBU composites tested showed an initial burst release within the first 5 minutes
391 that corresponds to the release of IBU from the edges and external surfaces of the LDH particles
392 [31,50]. The initial release is greatest with MgFe-LDH-IBU(co), which may indicate that the majority
393 of its IBU was associated with the outer surfaces of this LDH. This is supported by the pXRD
394 analysis that revealed poorer crystallinity compared to the other composites. MgFe-LDH-IBU(ex)
395 showed limited release, which suggests most of the IBU available for release was relinquished in
396 the initial burst phase. pXRD of this LDH did not suggest any IBU was intercalated but had adhered
397 onto the outer surfaces of the LDH.

398 A slower release rate of IBU followed the initial burst and corresponds to the phosphate ions
399 in the solution exchanging with the adsorbed IBU. LDHs are semi-rigid lamellar solids and
400 demonstrate a reduction in interlayer spacing when larger anions are exchanged with the smaller
401 anions [31]. As the intercalated IBU is exchanged for phosphate ions at the outer edges the
402 interlayer space reduces, inhibiting exchange with IBU deeper within the LDH structure. This can
403 explain the slow and partial release of IBU in anionic-exchanged LDHs as they have more crystalline
404 layers. Co-precipitated and anionic-exchanged MgAl-LDH-IBU have similar crystallinity, which may
405 explain their similar release profiles.

406 It is also likely that differences in the chemical composition and charge density of LDH layers
407 will affect the strength of interaction with IBU and therefore affect how easily the IBU can be
408 liberated thereafter [9,33]. Extrapolating this theory would suggest that IBU was held most
409 strongly within anionic-exchanged composites, especially MgFe-LDH-IBU(ex), and less strongly
410 within co-precipitated composites.

411 It is also proposed that H_2PO_4^- reacts with exposed hydroxyl groups of LDHs to produce a
412 hydroxyphosphate [51]. This is known as a solid state grafting reaction which obstructs IBU release
413 from deep within the layers due to the strong bonds between phosphate ions and cationic LDH
414 layers [50,51].

415 The release of IBU from MgAl-LDH-IBU was also studied by Ambrogi *et al.* [31], who
416 established modified release of IBU. The release rate of IBU from MgAl-LDH-IBU was found to be
417 60% over 20 minutes, which is similar to the data presented here showing 54% drug released over
418 the first 20 minutes. This demonstrates MgAl-LDH can be used as IBU drug carriers for modified
419 release.

420

421 **4. Conclusion**

422 IBU intercalates into LDHs by interaction between its negatively charged carboxylic acid group
423 and the cationic surface of the LDHs. Anionic-exchange of IBU onto a formed LDH generally
424 produces more crystalline and ordered materials compared to co-precipitating the LDH with IBU.
425 Intercalated IBU is initially released rapidly from the LDHs outer surfaces, then more slowly by ion-
426 exchange with phosphate ions in the dissolution medium. Formation of LDH-IBU composites via
427 ion exchange generally results in slower, partial, drug release compared to its co-precipitated
428 counterparts, which may be explained by intensity of LDU and IBU interactions.

429 The chemical composition of LDHs affects the crystallinity of the overall particle structure,
430 which affects the intercalation of IBU and its subsequent release profile. Mg^{2+} and Al^{3+} ions form
431 the most crystalline LDHs. The substitution of Mg^{2+} cations with higher charge-density Ni^{2+} cations
432 makes it difficult to synthesise LDH layers. Substitution of Al^{3+} cation with Fe^{3+} cation distorts the
433 layers due to its larger atomic radius. Therefore, Mg^{2+} and Al^{3+} ions were found to have the best
434 charge densities to form the cationic layers of LDHs.

435 This study demonstrates that MgAl-LDH has the optimal metal composition of LDHs to act as a
436 host for modifying release of IBU out of the four LDHs synthesised. Further research into the use of
437 MgAl-LDH as a drug carrier could yield interesting and promising materials for optimising patient
438 care.

439

440 **5. Future perspectives**

441 The arena of drug delivery is vast and ever expanding with novel approaches, materials and
442 technologies emerging from the research. This is justified by the extensive requirements for
443 modern drug delivery vehicles to improve patient outcomes, support adherence to medicines, and
444 reduce adverse effects. There are a large number of promising materials being investigated and
445 applied to the field, each with their set of desirable physicochemical and biological properties.
446 Current knowledge of the LDH materials provides an understanding of their chemical diversity and
447 the adaptability of their physical properties. It is this diversity which is the foundation of their
448 exploitation in biomedical applications.

449 The particle size dependent cellular uptake demonstrated by LDH materials make them
450 particularly interesting for drug delivery [52]. Further exploration of the biocompatibility,
451 pharmacokinetics and toxicity of LDH-drug hybrids [53] is required before their true potential is
452 acknowledged and advances made. The benefits of combining drug molecules with LDHs range
453 from improved drug solubility and bioavailability to overcoming drug resistance. Thus, utilising
454 such inorganic materials as novel delivery vehicles provides a platform for not only reducing the
455 use of animal and petroleum based materials in such applications but provides scope for bettering
456 the therapeutic effect of the drug molecules themselves.

457 In addition to delivery of drugs, the application of these low-cost materials extends to other
458 fields of biomedicine including LDH-polymer scaffolds for improved cell regeneration [12], LDH-
459 immobilised enzyme biosensors [54] as well as gene delivery vectors [55] further widening the
460 importance of research into these inorganic layered materials.

461

462 **6. Executive Summary**

463 Intercalation of ibuprofen in LDHs

- 464 • Adsorption of IBU into LDHs was achieved via co-precipitation and anion exchange.
- 465 • Co-precipitation of LDHs with IBU produced a lower yield than without IBU, implying larger
466 anions may inhibit successful formation of LDH layers.
- 467 • The co-precipitation of LDHs with IBU resulted in considerably higher drug intercalation
468 efficiencies and a stronger adsorption of IBU compared to the anion-exchanged counterparts.

469 Characterisation of LDHs

- 470 • FT-IR spectra and pXRD confirmed the intercalation of IBU within the lamellar structure of
471 MgAl-LDH and MgFe-LDH. An ordered layered structure for NiAl-LDH and NiFe-LDH was not
472 formed.

473 Drug release

- 474 • LDH chemical composition and IBU intercalation method also affected the final drug release
475 behaviour.
- 476 • An initial burst release was observed for all LDH-IBU composites within the first 5 minutes that
477 corresponds to the release of IBU from the edges and external surfaces of the LDH particles

- 478 • A slower release rate of IBU followed the initial burst and corresponds to the phosphate ions
479 in the solution exchanging with the adsorbed IBU.

480

481 **7. Acknowledgements:**

482 None

483

484 **8. Disclosures:**

485 None

486

487 **9. Ethical conduct of research statement**

488 Not applicable

489

490 **10. References**

491 Papers of special note have been highlighted as:

492 * of interest

493 ** of considerable interest

494 **1. Forano C, Costantino U, Prevott V, Taviot Gueho C. Layered Double Hydroxides (LDH). In:**
495 ***Handbook of Clay Science: Techniques and applications. Part B, Part 2.* Bergaya F, Lagaly G**
496 **(Eds.). . Elsevier, Amsterdam, 745–782 (2013).**

497 ** This book chapter provides an extensive overview of LDH materials, covering the synthesis, structure,
498 chemical and physical properties.

499 **2. Wong MS. Book Review: Multiple Choice Questions in Plastic Surgery. *Aesthetic Surg. J.***
500 **30(4), 632–633 (2010).**

501 **3. del Arco M, Fernández A, Martín C, Rives V. Release studies of different NSAIDs**
502 **encapsulated in Mg,Al,Fe-hydrotalcites. *Appl. Clay Sci.* 42(3–4), 538–544 (2009).**

503 **4. Rives V, Del Arco M, Martín C. Layered double hydroxides as drug carriers and for**
504 **controlled release of non-steroidal antiinflammatory drugs (NSAIDs): A review. *J. Control.***
505 ***Release.* 169(1–2), 28–39 (2013).**

506 **5. Djaballah R, Bentouami A, Benhamou A, Boury B, Elandalousi EH. The use of Zn-Ti**
507 **layered double hydroxide interlayer spacing property for low-loading drug and low-dose**
508 **therapy. Synthesis, characterization and release kinetics study. *J. Alloys Compd.* 739, 559–**
509 **567 (2018).**

510 **6. Rodrigues LADS, Figueiras A, Veiga F, et al. The systems containing clays and clay minerals**
511 **from modified drug release: a review. *Colloids Surf. B. Biointerfaces.* 103, 642–51 (2013).**

512 **7. Cavani F, Trifiro F, Vaccari A. Hydrotalcite-type anionic clays: preparation, properties and**
513 **applications. *Catal. Today.* 11, 173–301 (1991).**

514 **8. Zhang K, Xu ZP, Lu J, et al. Potential for layered double hydroxides-based, innovative drug**
515 **delivery systems. *Int. J. Mol. Sci.* 15(5), 7409–7428 (2014).**

516 **9. Williams GR, O’Hare D. Towards understanding, control and application of layered double**
517 **hydroxide chemistry. *J. Mater. Chem.* 16(30), 3065 (2006).**

518 * Review article outlining the chemistry of LDH synthesis and potential for applications of such
519 multifunctional materials.

520 **10. Bugatti V, Gorrasi G, Montanari F, Nocchetti M, Tammaro L, Vittoria V. Modified layered**
521 **double hydroxides in polycaprolactone as a tunable delivery system: in vitro release of**
522 **antimicrobial benzoate derivatives. *Appl. Clay Sci.* 52(1–2), 34–40 (2011).**

523 **11. Gu Z, Yan S, Cheong S, et al. Layered double hydroxide nanoparticles: Impact on vascular**
524 **cells, blood cells and the complement system. *J. Colloid Interface Sci.* 512, 404–410 (2018).**

525 **12. Fayyazbakhsh F, Solati-Hashjin M, Keshtkar A, Shokrgozar MA, Dehghan MM, Larijani B.**
526 **Novel layered double hydroxides-hydroxyapatite/gelatin bone tissue engineering**
527 **scaffolds: Fabrication, characterization, and in vivo study. *Mater. Sci. Eng. C.* 76, 701–714**
528 **(2017).**

529 **13. Wang F, Zhang Y, Liang W, Chen L, Li Y, He X. Non-enzymatic glucose sensor with high**
530 **sensitivity based on Cu-Al layered double hydroxides. *Sensors Actuators, B Chem.***
531 **273(January), 41–47 (2018).**

532 **14. Nath J, Dolui SK. Applied Clay Science Synthesis of carboxymethyl cellulose-g-poly (acrylic**

- 533 acid)/ LDH hydrogel for in vitro controlled release of vitamin B 12. *Appl. Clay Sci.*
534 155(February), 65–73 (2018).
- 535 15. Posati T, Giuri D, Nocchetti M, *et al.* Keratin-hydroxycalcites hybrid films for drug delivery
536 applications. *Eur. Polym. J.* 105(January), 177–185 (2018).
- 537 16. Barkhordari S, Yadollahi M. Carboxymethyl cellulose capsulated layered double
538 hydroxides/drug nanohybrids for Cephalexin oral delivery. *Appl. Clay Sci.* 121–122, 77–85
539 (2016).
- 540 17. Chubar N, Gerda V, Megantari O, *et al.* Applications versus properties of Mg-Al layered
541 double hydroxides provided by their syntheses methods: Alkoxide and alkoxide-free sol-
542 gel syntheses and hydrothermal precipitation. *Chem. Eng. J.* 234, 284–299 (2013).
- 543 18. Meng Z, Zhang Y, Zhang Q, *et al.* Novel synthesis of layered double hydroxides (LDHs)
544 from zinc hydroxide. *Appl. Surf. Sci.* 396, 799–803 (2017).
- 545 * Research article reports a new transformation synthesis method for preparation of LDH materials.
- 546 19. Berber MR, Minagawa K, Katoh M, Mori T, Tanaka M. Nanocomposites of 2-arylpropionic
547 acid drugs based on Mg-Al layered double hydroxide for dissolution enhancement. *Eur. J.*
548 *Pharm. Sci.* 35(4), 354–60 (2008).
- 549 20. Rojas R, Palena MC, Jimenez-Kairuz AF, Manzo RH, Giacomelli CE. Modeling drug release
550 from a layered double hydroxide–ibuprofen complex. *Appl. Clay Sci.* 62–63, 15–20 (2012).
- 551 21. Wei M, Pu M, Guo J, *et al.* Intercalation of L -Dopa into Layered Double Hydroxides :
552 Enhancement of Both Chemical and Stereochemical Stabilities of a Drug through Host-
553 Guest Interactions. *Chem. Mater.* 20(16), 5169–5180 (2008).
- 554 22. Xia S-J, Ni Z-M, Xu Q, Hu B-X, Hu J. Layered double hydroxides as supports for
555 intercalation and sustained release of antihypertensive drugs. *J. Solid State Chem.* 181(10),
556 2610–2619 (2008).
- 557 23. Tammaro L, Costantino U, Bolognese A, *et al.* Nanohybrids for controlled antibiotic
558 release in topical applications. *Int. J. Antimicrob. Agents.* 29(4), 417–23 (2007).
- 559 24. Zhao H, Zhang X. Enhanced apoptosis and inhibition of gastric cancer cell invasion
560 following treatment with LDH@Au loaded Doxorubicin. *Electron. J. Biotechnol.* 32, 13–18
561 (2018).
- 562 25. Choy J, Choi S, Oh J, Park T. Clay minerals and layered double hydroxides for novel
563 biological applications. *Appl. Clay Sci.* 36(1–3), 122–132 (2007).
- 564 * Review discusses the range of applications for LDH-biomaterial hybrid materials including
565 pharmaceutical, cosmetic, agricultural and environmental.
- 566 26. Day RO, Graham GG. Non-steroidal anti-inflammatory drugs (NSAIDs). *BMJ.* 346(June), 1–
567 7 (2013).
- 568 27. Fini A, Fazio G, Feroci G. Solubility and solubilization properties of non-steroidal anti-
569 inflammatory drugs. *Int. J. Pharm.* 126(1–2), 95–102 (1995).
- 570 28. Capsoni D, Quinzeni I, Bruni G, Friuli V, Maggi L, Bini M. Improving the Carprofen
571 Solubility: Synthesis of the Zn₂Al-LDH Hybrid Compound. *J. Pharm. Sci.* 107(1), 267–272
572 (2018).
- 573 * Recent article outlining findings of improved solubility of an NSAID drug when delivered as a hybrid
574 compound intercalated into a LDH material.
- 575 29. del Arco M, Fernández A, Martín C, Rives V. Solubility and release of fenbufen
576 intercalated in Mg, Al and Mg, Al, Fe layered double hydroxides (LDH): The effect of
577 Eudragit® S 100 covering. *J. Solid State Chem.* 183(12), 3002–3009 (2010).

- 578 30. Grubel P, Bhashar KR, Cave DR, Garik P, Stanley HE, Lamont JT. Interaction of an
579 aluminium-magnesium containing antacid and gastric mucus: possible contribution to the
580 cytoprotective function of antacids. *Aliment. Pharmacol. Ther.* 11(1), 139–145 (1997).
- 581 31. Ambrogi V, Fardella G, Grandolini G, Perioli L. Intercalation compounds of hydrotalcite-
582 like anionic clays with antiinflammatory agents--I. Intercalation and in vitro release of
583 ibuprofen. *Int. J. Pharm.* 220(1–2), 23–32 (2001).
- 584 32. Li B, He J, Gevans D, Duan X. Inorganic layered double hydroxides as a drug delivery
585 system?intercalation and in vitro release of fenbufen. *Appl. Clay Sci.* 27(3–4), 199–207
586 (2004).
- 587 33. del Arco M, Gutiérrez S, Martín C, Rives V, Rocha J. Synthesis and characterization of
588 layered double hydroxides (LDH) intercalated with non-steroidal anti-inflammatory drugs
589 (NSAID). *J. Solid State Chem.* 177(11), 3954–3962 (2004).
- 590 34. Harrison R, Li L, Gu Z, Xu ZP. Controlling mesoporous silica-coating of layered double
591 hydroxide nanoparticles for drug control release. *Microporous Mesoporous Mater.* 238,
592 97–104 (2017).
- 593 35. Reichle WT. Synthesis of anionic clay minerals (mixed metal hydroxides,hydrotalcite).
594 *Solid States Ionics.* 22, 135–141 (1986).
- 595 36. Djebbi MA, Bouaziz Z, Elabed A, *et al.* Preparation and optimization of a drug delivery
596 system based on berberine chloride-immobilized MgAl hydrotalcite. *Int. J. Pharm.* 506(1–
597 2), 438–448 (2016).
- 598 37. del Arco M, Cebadera E, Gutiérrez S, *et al.* Mg,Al layered double hydroxides with
599 intercalated indomethacin: synthesis, characterization, and pharmacological study. *J.*
600 *Pharm. Sci.* 93(6), 1649–58 (2004).
- 601 38. San Román MS, Holgado MJ, Salinas B, Rives V. Characterisation of Diclofenac, Ketoprofen
602 or Chloramphenicol Succinate encapsulated in layered double hydroxides with the
603 hydrotalcite-type structure. *Appl. Clay Sci.* 55, 158–163 (2012).
- 604 39. Gordijo CR, Barbosa C a S, Da Costa Ferreira AM, Constantino VRL, de Oliveira Silva D.
605 Immobilization of ibuprofen and copper-ibuprofen drugs on layered double hydroxides. *J.*
606 *Pharm. Sci.* 94(5), 1135–48 (2005).
- 607 40. Mendieta S, Nuñez PR, Oliva M, Pérez C, Fernández J, Crivello M. Intercalation of Anti-
608 inflammatory Drugs Sodium Indomethacin into Nanocomposites of Mg-Al. Structural
609 Characterization. *Procedia Mater. Sci.* 1, 580–587 (2012).
- 610 41. Rives V, del Arco M, Martín C. Intercalation of drugs in layered double hydroxides and
611 their controlled release: A review. *Appl. Clay Sci.* 88–89, 239–269 (2014).
- 612 ** Article outlines the intercalation of a wide range of drug molecules into LDH materials, including
613 antibiotics, anticancer drugs, vitamins, lipid regulating drugs, antidiabetic drugs, antifibrinolytic,
614 antihypertensive, and anticoagulant agents amongst others.
- 615 42. Miyata S. The Syntheses of Hydrotalcite-Like Compounds and Their Structures and
616 Physico-Chemical Properties I: The Systems Mg²⁺-Al³⁺-NO₃⁻, Mg²⁺-Al³⁺-Cl⁻, Mg²⁺-Al³⁺-
617 ClO₄⁻, Ni²⁺-Al³⁺-Cl⁻ and Zn²⁺-Al³⁺-Cl⁻. *Clays Clay Miner.* 23(5), 369–375 (1975).
- 618 43. Huang W, Zhang H, Pan D. Study on the release behavior and mechanism by monitoring
619 the morphology changes of the large-sized drug-LDH nanohybrids. *AIChE J.* 57(7), 1936–
620 1946 (2011).
- 621 44. Gasser MS. Inorganic layered double hydroxides as ascorbic acid (vitamin C) delivery
622 system--intercalation and their controlled release properties. *Colloids Surf. B.*

- 623 *Biointerfaces*. 73(1), 103–9 (2009).
- 624 45. Tao Q, Reddy BJ, He H, Frost RL, Yuan P, Zhu J. Synthesis and infrared spectroscopic
625 characterization of selected layered double hydroxides containing divalent Ni and Co.
626 *Mater. Chem. Phys.* 112(3), 869–875 (2008).
- 627 46. Hong N, Song L, Wang B, *et al.* Co-precipitation synthesis of reduced graphene oxide/NiAl-
628 layered double hydroxide hybrid and its application in flame retarding poly(methyl
629 methacrylate). *Mater. Res. Bull.* 49, 657–664 (2014).
- 630 47. del Arco M, Malet P, Trujillano R, Rives V. Synthesis and Characterization of Hydrotalcites
631 Containing Ni(II) and Fe(III) and Their Calcination Products. *Chem. Mater.* 11(3), 624–633
632 (1999).
- 633 48. Raja T. Physico-chemical studies on synthetic disordered Ni-Fe layered double hydroxides.
634 *J. Mater. Sci. Lett.* 15, 718–720 (1996).
- 635 49. Kubo D, Tadanaga K, Hayashi A, Tatsumisago M. Hydroxide ion conduction in Ni-Al layered
636 double hydroxide. *J. Electroanal. Chem.* 671(3), 102–105 (2012).
- 637 50. Perioli L, Posati T, Nocchetti M, Bellezza F, Costantino U, Cipiciani A. Intercalation and
638 release of antiinflammatory drug diclofenac into nanosized ZnAl hydrotalcite-like
639 compound. *Appl. Clay Sci.* 53(3), 374–378 (2011).
- 640 51. Costantino U, Casciola M, Massinelli L, Nocchetti M, Vivani R. Intercalation and grafting of
641 hydrogen phosphates and phosphonates into synthetic hydrotalcites and a.c.-conductivity
642 of the compounds thereby obtained. 97, 203–212 (1997).
- 643 52. Choi G, Kim TH, Oh JM, Choy JH. Emerging nanomaterials with advanced drug delivery
644 functions; focused on methotrexate delivery. *Coord. Chem. Rev.* 359, 32–51 (2018).
- 645 53. Choi SJ, Choy JH. Layered double hydroxide nanoparticles as target-specific delivery
646 carriers: uptake mechanism and toxicity. *Nanomedicine*. 6(5), 803–814 (2011).
- 647 54. Yuan J, Xu S, Zeng HY, *et al.* Hydrogen peroxide biosensor based on chitosan/2D layered
648 double hydroxide composite for the determination of H₂O₂. *Bioelectrochemistry*. 123,
649 94–102 (2018).
- 650 55. Choy J-H, Kwak S-Y, Jeong Y-J, Park J. Inorganic layered double hydroxides as nonviral
651 vectors. *Angew. Chemie Int. Ed.* 39(22), 4041–4045 (2000).
- 652